Electric Field Control of Interfacial Ferromagnetism in $CaMnO_3/CaRuO_3$ Heterostructures

A. J. Grutter,[1] B. J. Kirby,[1] M. T. Gray,[2,3] C. L. Flint,[2,3] U. S. Alaan,[2,3] Y. Suzuki,[3,4] and J. A. Borchers[1]
[1]*NIST Center for Neutron Research, National Institute of Standards and Technology, Gaithersburg, Maryland 20899, USA*
[2]*Department of Materials Science and Engineering, Stanford University, Stanford, California 94305, USA*
[3]*Geballe Laboratory for Advanced Materials, Stanford University, Stanford, California 94305, USA*
[4]*Department of Applied Physics, Stanford University, Stanford, California 94305, USA*
(Received 13 February 2015; revised manuscript received 8 June 2015; published 23 July 2015)

New mechanisms for achieving direct electric field control of ferromagnetism are highly desirable in the development of functional magnetic interfaces. To that end, we have probed the electric field dependence of the emergent ferromagnetic layer at $CaRuO_3/CaMnO_3$ interfaces in bilayers fabricated on $SrTiO_3$. Using polarized neutron reflectometry, we are able to detect the ferromagnetic signal arising from a single atomic monolayer of $CaMnO_3$, manifested as a spin asymmetry in the reflectivity. We find that the application of an electric field of 600 kV/m across the bilayer induces a significant increase in this spin asymmetry. Modeling of the reflectivity suggests that this increase corresponds to a transition from canted antiferromagnetism to full ferromagnetic alignment of the Mn^{4+} ions at the interface. This increase from 1 μ_B to 2.5–3.0 μ_B per Mn is indicative of a strong magnetoelectric coupling effect, and such direct electric field control of the magnetization at an interface has significant potential for spintronic applications.

DOI: 10.1103/PhysRevLett.115.047601 PACS numbers: 77.55.Nv, 75.70.Cn

Direct electric field control of magnetism is among the most important goals in nanoscale magnetics research. Only recently has progress been made in exploring new pathways to giant magnetoelectric coupling effects [1–5]. To date, the most popular routes towards magnetoelectric coupling focused on heterostructures incorporating ferroelectrics and multiferroics such as $BaTiO_3$ or $BiFeO_3$ [2,4,6]. Magnetoelectric coupling in multiferroic structures often relies on voltage-induced distortions in one material to strain an adjacent magnetic film and alter the magnetic properties. Although this strategy has yielded promising results, successful attempts to induce magnetoelectric coupling without multiferroicity or magnetoelasticity remain relatively rare and include systems such as III-V semiconductors and cuprate-manganite interfaces [1–13].

Transition metal oxides are promising materials for magnetoelectric coupling since their ground states are a delicate balance of competing interactions that may be tuned electrostatically. The emergence of highly tunable interfacial magnetic states in transition metal oxide heterostructures provides a promising route towards magnetoelectric coupling [14–17]. We have previously investigated ferromagnetism at the interface between the antiferromagnetic insulator $CaMnO_3$ and the paramagnetic metal $CaRuO_3$ [14,18,19]. $CaRuO_3/CaMnO_3$ superlattices exhibit ferromagnetism tightly confined to the interface [14,20]. While measurements of the ferromagnetic layer thickness range from 1–4 unit cells, theoretical calculations and our recent results strongly favor a thickness of 1 unit cell [17–20]. Nanda *et al.* proposed that the ferromagnetism is stabilized by leakage of itinerant electrons from $CaRuO_3$ into the $CaMnO_3$, facilitating double exchange [20]. Competition between antiferromagnetic superexchange and interfacial double exchange is understood to result in canted antiferromagnetism with a net magnetization of 1 μ_B/Mn [20]. The canting angle between adjacent spins is predicted to be highly sensitive to changes in the interfacial electron leakage [20]. Doubling the electron leakage is expected to induce a transition from canted antiferromagnetism to ferromagnetism [20]. By using an applied voltage to drive $CaRuO_3$ conduction electrons into and out of the interface, it may be possible to control the ferromagnetism.

To achieve the desired density of mobile electrons at the interface, we must modify the interfacial charge transfer by approximately 4×10^{13} e^-/cm^2 [20]. Carrier density variations of this magnitude have been extensively explored in $LaAlO_3/SrTiO_3$ interfaces through backgating the $SrTiO_3$ substrate [21,22]. Because of the large dielectric constant of $SrTiO_3$, voltages as low as 300 V are expected to induce the desired effect [21–23]. Therefore, to explore magnetoelectric coupling at the $CaRuO_3/CaMnO_3$ interface we have fabricated a series of $CaMnO_3$(9 unit cells)/$CaRuO_3$(3 unit cells) bilayers on (100) $SrTiO_3$ substrates using pulsed laser ablation. The films were fabricated with a laser fluence of 0.9 J/cm^2 at 680 °C in 8 Pa of O_2. The bilayers were capped with a sputtered AuPd electrode to ensure field uniformity, as shown in Fig. 1(top). Because of the difficulty of characterizing ferromagnetism originating from a single atomic layer, a $[(CaMnO_3)_9/(CaRuO_3)_3]_{10}$ superlattice was also fabricated under identical conditions

and compared with past examples of $CaRuO_3/CaMnO_3$ multilayers [18]. As these superlattices have been demonstrated to be highly insensitive to strain or thickness, the superlattice magnetic properties are expected to well represent those of the bilayers [14,18]. The depositions of all samples were monitored *in situ* using reflection high-energy electron diffraction for quality and thickness control.

Atomic force micrographs (AFMs) of the bilayers revealed smooth, high-quality films consistent with past examples of $CaRuO_3/CaMnO_3$ [18]. Figure 1 (top) shows a plan view AFM of the sample surface after deposition of the $CaMnO_3$ layer. The $CaMnO_3$ surface onto which we deposited the $CaRuO_3$ is extremely smooth with well-defined atomic terraces and an rms roughness of 0.14 nm. The addition of an ultrathin $CaRuO_3$ layer does not significantly alter the surface quality, with an rms roughness of 0.24 nm. After depositing 20 nm of AuPd the surface roughness is approximately 0.5 nm, slightly in excess of a single perovskite unit cell.

Analysis of the superlattice revealed magnetic properties typical of $CaRuO_3/CaMnO_3$ superlattices. As shown in Fig. 1 (bottom), SQUID magnetometry yielded a Curie temperature (T_C) of 100 K and hysteresis loops which saturated at approximately 1 μ_B/Mn. The excellent agreement with previous $CaRuO_3/CaMnO_3$ interfaces is a strong indication that the bilayers will exhibit similar interfacial ferromagnetism. X-ray reflectivity of the superlattice provided additional confirmation of material and interface quality. Fitting of the x-ray data is consistent with the expected thickness and yields interfacial roughnesses of less than 0.5 nm [24].

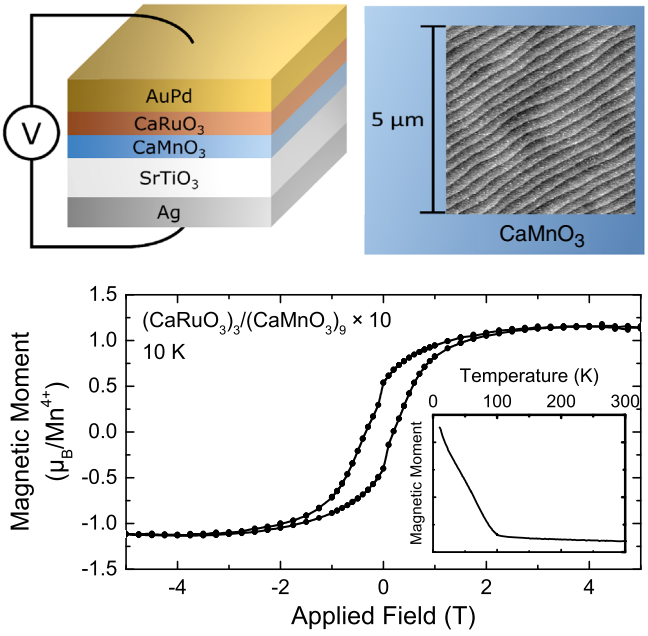

FIG. 1 (color online). (Top) Heterostructure schematic with plan view AFM of a typical bilayer after deposition of the $CaMnO_3$ layer. (Bottom) Magnetic hysteresis loop of a $[(CaRuO_3)_3/(CaMnO_3)_9]_{10}$ superlattice at 10 K. (Inset) Magnetization vs temperature of the same superlattice in an applied field of 20 mT after field cooling in 5 T.

Having demonstrated the interface quality and expected ferromagnetism in a superlattice, we characterized the magnetic properties of the gated bilayers. Unlike a superlattice in which nearly 20 magnetic interfaces enable the use of bulk measurement techniques, the ferromagnetic signal from a single interface falls below the noise floor of almost all magnetic characterization techniques. Additionally, any signal detected via bulk techniques would be too small to exclude alternative signal sources such as magnetic contamination. An ideal technique to penetrate a 20 nm electrode and detect such a small signal while remaining insensitive to magnetic contaminants is polarized neutron reflectometry (PNR), which probes the magnetic depth profile [31]. Therefore, we have performed comprehensive PNR measurements on a pair of $CaMnO_3/CaRuO_3$ bilayers, referred to as sample A and sample B, respectively.

Measurements were performed using the PBR (Polarized Beam Reflectometer) instrument at the NIST Center for Neutron Research. Sample A was cooled to 10 K in an applied magnetic field of 700 mT under bias voltages of −400 V and 0 V, where the bias voltage refers to the potential of the AuPd electrode relative to the backgate. Before each measurement, the sample was heated above T_C and cooled at the desired magnetic field and voltage bias. A second measurement was performed in which sample A was cooled to 10 K in 700 mT at −400 V. The voltage was then set to −400 V, 0 V, and +350 V without changing temperature. In a third measurement, we probed sample B after field cooling to 20 K in 700 mT and voltages of −300 V and 0 V, heating and recooling between voltages.

In all cases, incident and scattered neutrons were polarized either spin-up or spin-down with respect to the applied magnetic field. The specular reflectivity of spin-polarized neutrons is dependent on the depth profile of the sample magnetization parallel to the applied field, as well as the depth profile of the nuclear composition. Subtracting and normalizing the two non-spin-flip reflectivities, $R_{\uparrow\uparrow}$ and $R_{\downarrow\downarrow}$, yields the spin asymmetry (SA), which is dependent on the magnetization parallel to the applied field. Thus,

$$\mathrm{SA} = \frac{R_{\uparrow\uparrow} - R_{\downarrow\downarrow}}{R_{\uparrow\uparrow} + R_{\downarrow\downarrow}}, \tag{1}$$

where ↑ and ↓ refer to a neutron spin orientation parallel or antiparallel to the applied magnetic field, respectively. $R_{\uparrow\uparrow}$ refers to a neutron with spin parallel to the applied field both before and after scattering. PNR data were modeled using the REFL1D software package [32]. We note that all reasonable models of this system predict linear scaling

between the $CaMnO_3$ interfacial magnetization and the magnitude of the spin asymmetry [24]. Thus, although we explore numerous theoretical models throughout this work, our conclusions regarding magnetoelectric coupling are largely independent of the models, which primarily provide an additional quantitative scale and show consistency with the expected interfacial magnetization of the system [24].

The non-spin-flip reflectivities of sample A under a −400 V bias are shown in Fig. 2(a) along with a theoretical model. In all figures, error bars represent propagation of the uncertainty in counting statistics, $\sqrt{N}$. The spin asymmetries of sample A after cooling in 0 V and −400 V are shown in Figs. 2(b) and 2(c), respectively, while the nuclear and magnetic scattering length densities of the model used to fit the −400 V data appear in Fig. 2(d). This model consists of low-roughness $CaMnO_3$, $CaRuO_3$, AuPd, and an organic surface layer likely due to residual solvent originating in silver paint surface contacts. The AuPd electrode density is reduced near the $CaRuO_3$/AuPd interface, indicating a porous transitional growth region. Although the model is sensitive to the integrated $CaMnO_3$ magnetic moment, the narrow Q_Z range probed does not constrain the modeling sufficiently to distinguish tightly confined interfacial ferromagnetism from ferromagnetism spread throughout the $CaMnO_3$ layer [24]. Instead we rely on past studies of $CaRuO_3$/$CaMnO_3$ superlattices which demonstrated the interfacial nature of the magnetism [17,18]. A clear increase in the spin asymmetry is observed under a bias of −400 V, as demonstrated by Fig. 2(e) which focuses on a Q_Z range near the critical edge with low statistical uncertainty. Statistical testing shows a three σ deviation between the spin asymmetry curves of the two voltage states [24]. Taking the ratios of the two asymmetries reveals that splitting, and hence the magnetization, at −400 V is 2.86 ± 0.4 times the splitting at 0 V. This is consistent with the models shown in Fig. 2(e), corresponding to interface magnetizations of 0.97 and 2.64 μ_B/Mn for 0 V and −400 V, respectively.

To assess magnetization control at constant temperature rather than heating and cooling under different bias voltages, we performed a second measurement of sample A. We focused on a small Q_Z range (0.014–0.017) $Å^{-1}$ corresponding to the lowest-Q_Z peak in the spin asymmetry to maximize statistics with minimal counting time. Sample A was cooled to 10 K in a 700 mT field at a bias voltage of −400 V, and the voltage was varied between −400 V, 0 V, and +350 V at constant temperature. The results are plotted in Fig. 2(f), which shows a difference between the positive and negative bias states. Integrating the peak intensity for each bias condition yields Fig. 2(f) (inset), which shows a decrease in spin asymmetry as the bias voltage is reversed. Thus, we find magnetoelectric coupling at constant temperature in which the interfacial magnetization is reduced by the application of a positive voltage.

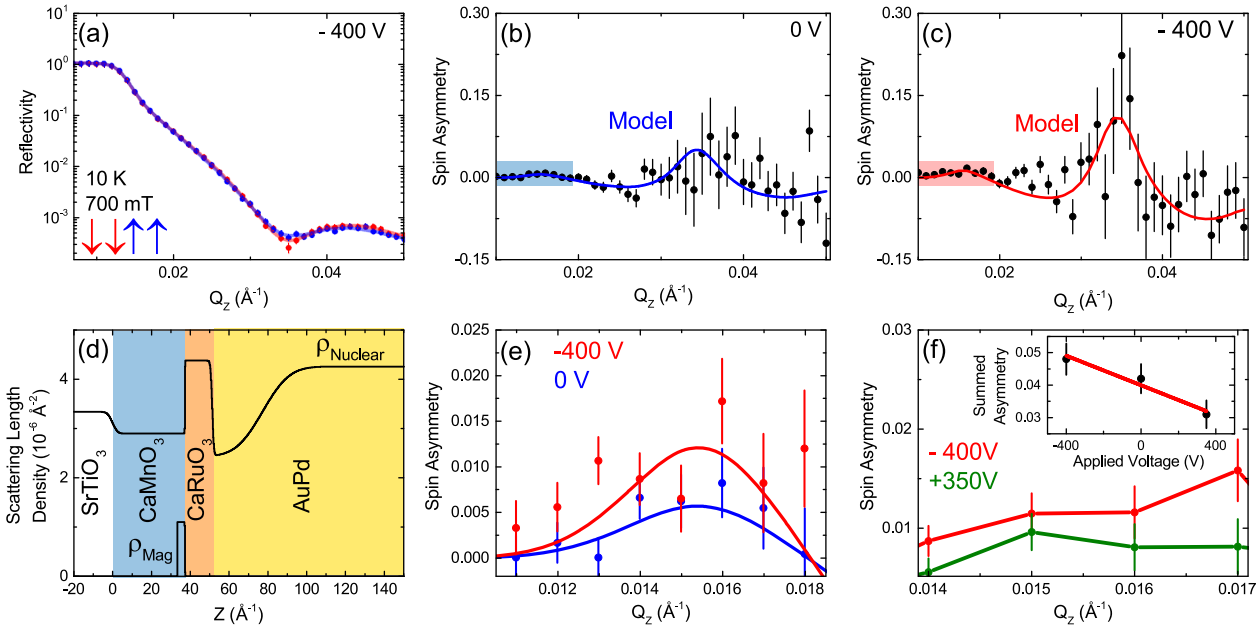

FIG. 2 (color online). (a) Spin dependent reflectivity of sample A after cooling to 10 K in 700 mT under a −400 V bias. The solid lines represent a model fit to the data. (b) Spin asymmetry of sample A after cooling in 700 mT without a bias. (c) Spin asymmetry of sample A after cooling in 700 mT with a bias of −400 V. Solid lines in (b) and (c) are spin asymmetries predicted by modeling. (d) Nuclear and magnetic depth profile used to model sample A at −400 V. (e) Close-up of the highlighted regions of (b) and (c). (f) Spin asymmetry of sample A after cooling in −400 V and 700 mT and varying bias voltage at constant temperature. The measured region corresponds to the FWHM of the spin asymmetry peak shown in part (e). (Inset) Summation of the spin asymmetry of the peak in (f) as a function of applied voltage.

Although it is challenging to extract precise magnetization values from such a small Q_Z range, we estimate the interface magnetization to be approximately 2.7 ± 0.3, 2.0 ± 0.25, and 1.4 ± 0.2 μ_B/Mn at −400, 0, and +350 V, respectively. Although measurement at constant temperature yields a smaller effect than heating and recooling, the difference in spin asymmetry is a 4.8σ event and conclusively demonstrates magnetoelectric coupling.

Finally, voltage dependent measurements of sample B in Fig. 3 show interfacial magnetization trends which are nearly identical to those of sample A. In this case measuring a larger Q_Z range allowed the detection of additional peaks in the spin asymmetry. Consequently oscillations are observed out to 0.1 Å^{-1}. A χ^2 test shows a three σ deviation between the spin asymmetry curves of the two voltage states (0 V and −300 V). Although in this case the complex nature of the AuPd electrode precludes a precise, unique fit to the full reflectivity curve, we may easily reproduce the spin asymmetry at −300 V using a simple toy model, shown as a guide to the eye (black line) which includes the low-roughness $CaMnO_3$, $CaRuO_3$, and AuPd at the expected thicknesses and one interfacial unit cell of magnetic $CaMnO_3$ with a magnetization of 2.54 μ_B/Mn. In contrast, the 0 V state lacks any statistically significant peaks in the spin asymmetry. The expected magnetization of 1 μ_B/interfacial Mn (or smaller) is consistent with the measurement, but not with larger magnetization values. Given the increase in spin asymmetry for the −300 V measurement shown in Fig. 3(b), we find an increase by a factor of 2.5 to 3 over the values reported in previous studies of $CaRuO_3$/$CaMnO_3$ interfaces [18]. Thus, the high-voltage state is consistent with a transition from canted antiferromagnetism to ferromagnetism at the interface. With three such statistically significant measurements, we may now be confident that applying an electric field changes the magnetic depth profile of $CaRuO_3$/$CaMnO_3$ bilayers, increasing the field cooled magnetization at the interface from 0.75–1 μ_B/Mn to 2.5–3.0 μ_B/Mn.

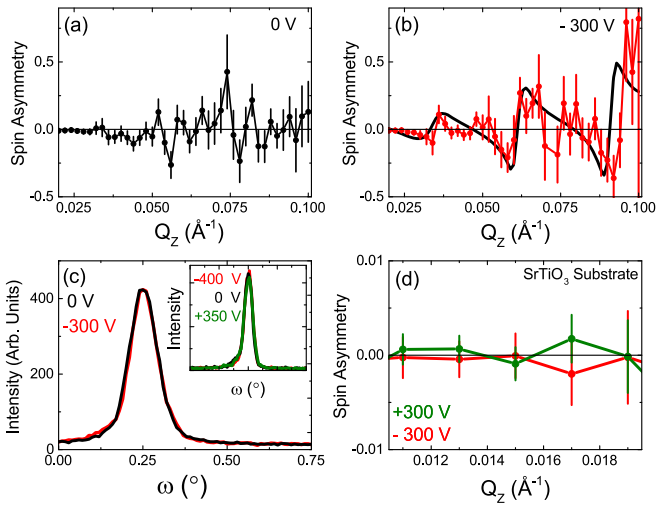

FIG. 3 (color online). Spin asymmetry of sample B as a function of Q_Z under a voltage of (a) 0 V and (b) −300 V. Sample was field cooled to 20 K in a field of 700 mT. The black line in (b) is a guide to the eye based on a simple toy model with a magnetization of 2.54 μ_B/Mn in a single unit cell of $CaMnO_3$ at the interface. (c) Specular reflection rocking curves after cooling in 0 V and −300 V. (inset) Specular reflection rocking curves at a constant temperature of 10 K for voltages of −400, 0, and +350 V. (d) Spin asymmetry of an identically measured $SrTiO_3$ substrate at −300 V and +300 V.

Although we have clearly demonstrated voltage dependent spin asymmetry, such small signals must be carefully evaluated to eliminate possible sources of error and establish statistical significance. We therefore considered alternative explanations for the observed effect, including the effects of leakage current, single-phase magnetoelectricity, and electrostriction [24]. Based on the lack of any observable leakage current, the weak nature of single-phase magnetoelectric coupling, and the lack of a strongly magnetostrictive material in the system, we conclude that none of these effects can be responsible [4,24,33–36]. To ensure that no time dependent effects altered the results, zero-bias voltage measurements were performed both before and after the application of a large negative bias voltage, and no difference is observed based on measurement order. Additionally, the changes in spin asymmetry were persistent regardless of background subtraction and polarization correction [24].

Cooling under different electric fields did not alter the structural features of the reflectivity, allowing for robust comparisons between the two states. Such structural stability starkly contrasts with electric field dependent measurements performed on piezoelectric and ferroelectric substrates, in which an applied electric field is well known to alter the surface geometry in addition to any structural distortions which may be induced [4,37]. Such surface modifications are known to significantly affect the neutron reflectivity rocking curve. Additionally, although the large $SrTiO_3$ dielectric was critical to enhancing interfacial charge transfer and enabled modulation of magnetism in $CaMnO_3$/$CaRuO_3$ bilayers, the $SrTiO_3$ surface may form facets below its structural transition at 105 K. Faceting may alter the reflectivity and affect the width of the rocking curve. We therefore collected bilayer rocking curves after cooling at different bias voltages. As shown in Fig. 3(c), cooling under different voltages results in identical rocking curves. Figure 3(c) (inset) shows identical results for measurements taken at various voltages at 10 K. The primary structural scattering features are also extremely stable under all bias voltages. We therefore conclude that all changes in the reflectivity upon bias voltage application were magnetic in origin.

As an additional control test, we measured the reflectivity of a $SrTiO_3$ substrate capped by a sputtered Au

contact with similar thickness to the $CaMnO_3$/$CaRuO_3$/AuPd multilayers. The substrate was mounted and measured identically to that which has already been described, and the resulting spin asymmetry is shown in Fig. 3(d). We observe no spin asymmetry and no difference between the bias voltage states. Rather, the integrated deviation between the two curves for the region shown is 0.005 ± 0.009.

We conclude that a bias voltage tunes the ferromagnetic interface which forms in $CaMnO_3/CaRuO_3$ heterostructures. This control is explained in terms of driving conduction electrons from the $CaRuO_3$ across the interface into the $CaMnO_3$, where an enhanced interfacial double exchange interaction manifests as an increase of the magnetization by a factor of 2.86 ± 0.4, from an initial unbiased value of 0.75–1 μ_B per interfacial Mn at 0 V to 2.5–3.0 μ_B per interfacial Mn at an applied potential of −300 V or −400 V. We have also demonstrated real-time control of the magnetization enhancement. It should finally be noted that, although we conclusively report an enhancement of the magnetization, we do not definitively determine the thickness of the ferromagnetic layer upon application of a bias voltage. These findings represent a new route towards direct, functionalizable electric field control of magnetism at the nanoscale, underscoring once more the promise of emergent magnetic properties in complex oxide heterostructures.

The authors would like to thank Tanya Dax and Dr. Aurora Alberca for their work on sample environment with voltage application. Neutron scattering was performed at the NIST Center for Neutron Research. Research at Stanford was supported by the U.S. Department of Energy, Director, Office of Science, Office of Basic Energy Sciences, Division of Materials Sciences and Engineering under Contract No. DESC0008505.

[1] R. Cherifi *et al.*, Nat. Mater. **13**, 345 (2014).
[2] G. Radaelli *et al.*, Nat. Commun. **5**, 3404 (2014).
[3] F. A. Cuellar *et al.*, Nat. Commun. **5**, 4215 (2014).
[4] W. Eerenstein, M. Wiora, J. L. Prieto, J. F. Scott, and N. D. Mathur, Nat. Mater. **6**, 348 (2007).
[5] S. Zhang *et al.*, Phys. Rev. Lett. **108**, 137203 (2012).
[6] J. T. Heron, D. G. Schlom, and R. Ramesh, Appl. Phys. Rev. **1**, 021303 (2014).
[7] D. Chiba, M. Sawicki, Y. Nishitani, Y. Nakatani, F. Matsukura, and H. Ohno, Nature (London) **455**, 515 (2008).
[8] D. Chiba, F. Matsukura, and H. Ohno, Appl. Phys. Lett. **89**, 162505 (2006).
[9] C. H. Ahn *et al.*, Rev. Mod. Phys. **78**, 1185 (2006).
[10] M. Zhernenkov, M. R. Fitzsimmons, J. Chlistunoff, J. Majewski, I. Tudosa, and E. E. Fullerton, Phys. Rev. B **82**, 024420 (2010).
[11] M. Weisheit, S. Fahler, A. Marty, Y. Souche, C. Poinsignon, and D. Givord, Science **315**, 349 (2007);
[12] D. Chiba, S. Fukami, K. Shimamura, N. Ishiwata, K. Kobayashi, and T. Ono, Nat. Mater. **10**, 853 (2011).
[13] C. Bi, Y. Liu, T. Newhouse-Illige, M. Xu, M. Rosales, J. W. Freeland, O. Mryasov, S. Zhang, S. G. E. te Velthuis, and W. G. Wang, Phys. Rev. Lett. **113**, 267202 (2014).
[14] K. S. Takahashi, M. Kawasaki, and Y. Tokura, Appl. Phys. Lett. **79**, 1324 (2001).
[15] K. Ueda, T. Hitoshi, and T. Kawai, Science **280**, 1064 (1998).
[16] M. Gibert *et al.*, P. Zubko, R. Scherwitzl, J. Íñiguez, and J.-M. Triscone, Nat. Mater. **11**, 195 (2012).
[17] A. Grutter *et al.*, Phys. Rev. Lett. **111**, 087202 (2013).
[18] C. He *et al.*, Phys. Rev. Lett. **109**, 197202 (2012).
[19] J. W. Freeland *et al.*, Phys. Rev. B **81**, 094414 (2010).
[20] B. R. K. Nanda, S. Satpathy, and M. S. Springborg, Phys. Rev. Lett. **98**, 216804 (2007).
[21] M. Ben Shalom, M. Sachs, D. Rakhmilevitch, A. Palevski, and Y. Dagan, Phys. Rev. Lett. **104**, 126802 (2010).
[22] M. Hosoda, Y. Hikita, H. Y. Hwang, and C. Bell, Appl. Phys. Lett. **103**, 103507 (2013).
[23] R. C. Neville *et al.*, J. Appl. Phys. **43**, 2124 (1972).
[24] See Supplemental Material at http://link.aps.org/supplemental/10.1103/PhysRevLett.115.047601 for additional details regarding X-ray reflectometry, modeling of the polarized neutron reflectometry, statistical analysis, and potential alternative sources of magnetoelectric coupling, which includes Refs. [25–30].
[25] V. J. Folen, G. T. Rado, and E. W. Stalder, Phys. Rev. Lett. **6**, 607 (1961).
[26] J. Ryu, A. Vazquez Carazo, K. Uchino, and H.-E. Kim, Jpn. J. Appl. Phys. **40**, 4948 (2001).
[27] S. Dong, J. Zhai, J. Li, and D. Viehland, Appl. Phys. Lett. **89**, 252904 (2006).
[28] I. A. Sergienko and E. Dagotto, Phys. Rev. B **73**, 094434 (2006).
[29] M. Fiebig, J. Phys. D **38**, R123 (2005).
[30] K. Momma and F. Izumi, J. Appl. Crystallogr. **44**, 1272 (2011).
[31] M. R. Fitzsimmons and C. F. Majkrzak, in *Modern Techniques for Characterizing Magnetic Materials*, edited by Z. Zhu (Kluwer, New York, 2005).
[32] B. J. Kirby, P. A. Kienzle, B. B. Maranville, N. F. Berk, J. Krycka, F. Heinrich, and C. F. Majkrzak, Curr. Opin. Colloid Interface Sci. **17**, 44 (2012).
[33] E. Bousquet and N. Spaldin, Phys. Rev. Lett. **107**, 197603 (2011).
[34] E. Ascher *et al.*, J. Appl. Phys. **37**, 1404 (1966).
[35] N. Hur, S. Park, P. A. Sharma, J. S. Ahn, S. Guha, and S.-W. Cheong, Nature (London) **429**, 392 (2004).
[36] T. Kimura, T. Goto, H. Shintani, K. Ishizaka, T. Arima, and Y. Tokura, Nature (London) **426**, 55 (2003).
[37] A. Alberca *et al.*, Phys. Rev. B **88**, 134410 (2013).